MRI Outperforms [18F]AV-1451 PET as a Longitudinal Biomarker in Progressive Supranuclear Palsy

Article *in* Movement Disorders · November 2018

DOI: 10.1002/mds.27546

12 authors, including:

Christopher G. Schwarz
Mayo Foundation for Medical Education and Research
169 PUBLICATIONS **1,993** CITATIONS
SEE PROFILE

Hugo Botha
Mayo Foundation for Medical Education and Research
75 PUBLICATIONS **565** CITATIONS
SEE PROFILE

Matthew L Senjem
Mayo Foundation for Medical Education and Research
405 PUBLICATIONS **13,814** CITATIONS
SEE PROFILE

Clifford R Jack
Mayo Foundation for Medical Education and Research
1,560 PUBLICATIONS **100,342** CITATIONS
SEE PROFILE

RESEARCH ARTICLE

MRI Outperforms [18F]AV-1451 PET as a Longitudinal Biomarker in Progressive Supranuclear Palsy

Jennifer L. Whitwell, PhD,[1*] Nirubol Tosakulwong, BS,[2] Christopher G. Schwarz, PhD,[1] Hugo Botha, MD,[3] Matthew L. Senjem, MS,[1,4] Anthony J. Spychalla, BS,[1] J. Eric Ahlskog, PhD, MD,[3] David S. Knopman, MD,[3] Ronald C. Petersen, MD, PhD,[3] Clifford R. Jack Jr. MD,[1] Val J. Lowe, MD[1] and Keith A. Josephs, MD, MST MSc[3]

[1]*Department of Radiology, Mayo Clinic, Rochester, Minnesota, USA*
[2]*Department of Health Sciences Research, Mayo Clinic, Rochester, Minnesota, USA*
[3]*Department of Neurology, Mayo Clinic, Rochester, Minnesota, USA*
[4]*Department of Information Technology, Mayo Clinic, Rochester, Minnesota, USA*

ABSTRACT: Background: Elevated uptake of the [^{18}F]AV-1451 tau-PET ligand has been observed cross-sectionally in subjects with progressive supranuclear palsy (PSP). However, it is unknown how the ligand performs longitudinally in PSP. We aimed to determine how regional measures of change on [^{18}F]AV-1451 PET perform as longitudinal biomarkers of PSP compared with the more established biomarker of rate of midbrain atrophy.

Methods: Sixteen subjects with PSP underwent 2 serial [^{18}F]AV-1451 tau-PET scans and 3-Tesla MRI over 12 months and were age- and sex-matched to 39 healthy controls with longitudinal [^{18}F]AV-1451 PET. Median [^{18}F]AV-1451 uptake was calculated for each scan for regions of interest across the brain and divided by uptake in cerebellar crus to create standard uptake value ratios. Midbrain volume on MRI was also calculated for each scan. Sample sizes required to power placebo-controlled treatment trials were calculated.

Results: Rate of midbrain atrophy was significantly increased in PSP compared with controls. [^{18}F]AV-1451 regional change measures were significantly increased in PSP compared with controls in the pallidum, precentral cortex, dentate nucleus of the cerebellum, and midbrain. Change over time in the PSP Rating Scale correlated with change in midbrain volume but did not correlate with change in the [^{18}F]AV-1451 measures. Smallest sample-size estimates were obtained with rate of midbrain atrophy, followed by the PSP Rating Scale, with both outperforming [^{18}F]AV-1451 measures.

Conclusions: [^{18}F]AV-1451 tau-PET measures increase over time in subjects with PSP, but longitudinal [^{18}F]AV-1451 measures may not perform as well as rate of midbrain atrophy as biomarkers for PSP clinical trials. © 2018 International Parkinson and Movement Disorder Society

Key Words: positron emission tomography; rates; Richardson's syndrome; serial; tau

Progressive supranuclear palsy (PSP) is a devastating neurodegenerative disease. Patients with PSP typically have difficulty with gait and posture, frequently fall, and have vertical supranuclear gaze palsy on neurological examination.[1,2] At autopsy, the vast majority of patients clinically diagnosed with PSP have deposition of 4-repeat tau[3-5]; hence, tau is a major target for future treatments of PSP, and PSP subjects are being targeted for clinical treatment trials for tau-based therapies. Hence, biomarkers that track disease progression in PSP are extremely valuable. At present, the most studied and validated biomarkers come from MRI,[6] with rate of midbrain atrophy confirmed as a reliable biomarker in PSP, which allows small sample-size estimates for clinical treatment trials.[7-9] However, MRI only provides a surrogate biomarker of underlying pathology. No disease-specific biomarker currently exists that can track progression of tau pathology during life that could be used as an outcome measure in treatment trials.

*Correspondence to: Jennifer L. Whitwell, PhD, Professor of Radiology, Department of Radiology, Mayo Clinic, 200 1st St. SW, Rochester, MN 55905; whitwell.jennifer@mayo.edu

Funding agencies: This study was funded by R01-NS89757, U01-AG006786, and R01-AG34676.

Relevant conflicts of interest/financial disclosures: The authors have no conflicts of interest.

Received: 1 May 2018; **Accepted:** 26 September 2018

Published online 00 Month 2018 in Wiley Online Library (wileyonlinelibrary.com). DOI: 10.1002/mds.27546

Positron emission tomography (PET) imaging using recently developed tau ligands such as [^{18}F]AV-1451[10,11] are therefore potentially important and may provide disease-specific in vivo biomarkers. Cross-sectional studies in PSP patients have demonstrated elevated uptake of [^{18}F]AV-1451, predominantly in subcortical regions, including the cerebellar dentate nucleus, midbrain, pallidum, thalamus, subthalamic nucleus, and striatum compared with controls, although it is unclear whether [^{18}F]AV-1451 uptake in these patients really reflects 4R tau pathology.[12-15] The majority of groups, with one exception,[16] have also found that [^{18}F]AV-1451 uptake in PSP does not correlate with clinical disease severity.[16-21]

[^{18}F]AV-1451 tau-PET could provide a biologically plausible biomarker of PSP disease progression. Obviously, it would be important to determine whether [^{18}F]AV-1451 tau-PET signal changes over time in PSP and correlates with clinical disease progression. Currently, it is unknown how [^{18}F]AV-1451 performs longitudinally in this disorder. Therefore, we aimed to assess longitudinal tau-PET using the [^{18}F]AV-1451 ligand in PSP subjects who had undergone serial scanning and compare the performance of [^{18}F]AV-1451 PET with the MRI-based biomarker of rate of midbrain atrophy. We hypothesized that [^{18}F]AV-1451 uptake in subcortical regions would increase over time in PSP and that [^{18}F]AV-1451 would perform comparably to midbrain atrophy in differentiating PSP subjects from controls.

Methods

Subjects

Sixteen subjects that fulfilled clinical criteria for probable PSP[2] underwent 2 serial [^{18}F]AV-1451 PET scans and accompanying 3 T MRI with follow-up intervals of approximately 12 months. All subjects had been identified from the Department of Neurology, Mayo Clinic, and consecutively recruited into an National Institutes of Health-funded prospective longitudinal PSP study by a neurodegenerative specialist and PSP expert (K.A.J.). All baseline evaluations occurred between February 18, 2015, and December 6, 2016, and follow-ups were completed between March 1, 2016, and December 5, 2017. Subjects were included in the study if they met criteria for probable PSP, had symptoms for ≤5 years, and were able to ambulate at least short distances independently. Of the 16 subjects, 14 fulfilled clinical criteria for PSP-Richardson's syndrome, 1 met criteria for PSP-parkinsonism, and 1 met criteria for PSP-progressive gait freezing.[2] Two subjects with PSP-Richardson's syndrome also met criteria for PSP-speech/language.[2] One subject has died and had pathologically confirmed PSP.

All subjects underwent clinical and neurological examinations and completed standardized and validated testing, including the PSP Rating Scale (PSPRS)[22] as a measure of clinical disease severity, the PSP Saccadic Impairment Scale[23] as a measure of eye movement abnormalities, the Montreal Cognitive Assessment (MoCA)[24] as a measure of global cognitive function, and the Frontal Assessment Battery[25] as a measure of executive function. Demographic and clinical features of the 16 PSP subjects are shown in Table 1.

The 16 PSP subjects were matched by age to 39 healthy control subjects who had undergone serial [^{18}F]AV-1451 imaging in the Mayo Clinic Study of Aging. The control cohort consisted of 18 female subjects (46%) with a mean education level ± standard deviation (SD) of 15 ± 2 years, mean age at tau-PET ± SD of 68 ± 8 years, mean follow-up interval ± SD of 1.29 ± 0.13 years, and mean MoCA of 26 ± 2. All control subjects were negative for beta-amyloid deposition on Pittsburgh Compound B PET.[26] The study was approved by the Mayo institutional review board. All subjects consented to the research.

Neuroimaging Analyses

Tau-PET imaging was performed using the [^{18}F]AV-1451 ligand and a PET/CT scanner (GE Healthcare, Milwaukee, WI). An intravenous bolus injection of approximately 370 MBq (range, 333-407 MBq) of [^{18}F]AV-1451 was administered, followed by a 20-minute PET acquisition performed 80 minutes after injection. Partial volume correction (PVC) of PET data was performed using a 2-compartment model.[27] All subjects had a 3 T MPRAGE sequence performed at the time of the tau-PET (TR/TE/T1, 2300/3/900 milliseconds; flip angle, 8°;

TABLE 1. Demographic and clinical features of the cohort

	PSP (n = 16)
Demographic data	
Women, n (%)	6 (40%)
Age at baseline, years	68 (6) [59, 83]
Age at onset, years	63 (6) [54, 80]
Scan interval, years	0.98 (0.10) [0.8, 1.2]
Disease duration at baseline, years	4.4 (1.7) [2.3, 8.9]
Clinical data	
PSP Rating Scale	
Baseline	36 (14) [9, 60]
Change/year	11.7 (6.5) [1.9, 23.2]
PSP Rating Scale — gait/midline	
Baseline	9 (6) [0, 15]
Change/year	3.1 (2.4) [0, 9.1]
PSP Saccadic Impairment Scale	
Baseline	2.6 (0.96) [1, 4]
Change/year	0.7 (0.75) [0, 2]
Montreal Cognitive Assessment Battery	
Baseline	26 (3) [19, 30]
Change/year	-1.6 (2.8) [3.5, -5.9]
Frontal Assessment Battery	
Baseline	15 (2) [12, 18]
Change/year	-0.8 (1.4) [1.2, -4]

Data are shown as mean (standard deviation) [min, max].

26-cm field of view; 256 × 256 in-plane matrix with a phase FOV of 0.94; slice thickness of 1.2 mm; in-plane resolution of 1 mm).

MPRAGE images were each segmented and corrected for intensity inhomogeneity using SPM12 Unified Segmentation[28] with modifications and tissue priors from the Mayo Clinic Adult Lifespan Template (MCALT; https://www.nitrc.org/projects/mcalt/).[29] Midbrain volume was measured for each scan by propagating a template-drawn midbrain volume mask into the native space of each patients scan and summing segmented per-voxel gray- and white-matter probabilities.[30] The template-drawn midbrain volume mask was traced using Analyze software (Biomedical Imaging Resource, Mayo Clinic, Rochester, MN) according to previously published guidelines.[31]

[^{18}F]AV-1451 images were each coregistered and resampled to the corresponding MPRAGE of the subjects using SPM12 6-degree-of-freedom rigid body registration and B-spline interpolation. All regions of interest were defined in MCALT space. The dentate nucleus of the cerebellum was defined as previously described[20] on MCALT, and voxels containing the dentate nucleus of the cerebellum were removed from all other cerebellar regions of interest. The midbrain volume mask described above[31] was transformed to MCALT. The Deep Brain Stimulation Intrinsic Template Atlas[32] was transformed into MCALT space and used to define regions for the subthalamic nucleus, red nucleus, and substantia nigra. All other regions of interest were defined using the MCALT atlas. For each subject MPRAGE, a nonlinear mapping to MCALT was created using Advanced Normaliation Tools,[33] and this mapping was used to automatically localize all regions on the native MPRAGE image using GenericLabel interpolation. Each region was then masked to include only gray- or white-matter-segmented voxels, and PET regional values were measured as the median image intensity across these voxels. Regional median values were divided by the median uptake in cerebellar crus gray matter to create standard uptake ratios (SUVRs). The crus region was selected to provide cerebellar gray matter in relative isolation from CSF spaces and to avoid being adjacent to parahippocampal, fusiform, and lingual gyri to avoid bleed-in signal from tau pathology.[34] Left and right hemisphere structures were combined for each region of interest. Manual quality control checks were performed on the [^{18}F]AV-1451 and MPRAGE scans, as well as on the segmentations and registrations of the atlas regions of interest onto the [^{18}F]AV-1451 scans. Two subjects were excluded from the MRI analysis because of motion artifacts on one of their MRI scans. However, all 16 subjects were included in the tau-PET analysis because the atlas-to-[^{18}F]AV-1451 registrations were acceptable.

An initial assessment of the longitudinal data was performed using 52 regions of interest across all cortical and subcortical structures. This allowed us to investigate general patterns in the data in an unbiased manner. A smaller, more specific set of regions was then used to assess rates of change in [^{18}F]AV-1451 uptake over time. The smaller set of 15 regions included 9 subcortical and brain stem regions that have been shown to have tau uptake in cross-sectional studies (midbrain, thalamus, dentate nucleus of the cerebellum, globus pallidus, caudate, putamen, subthalamic nucleus, substantia nigra, red nucleus) and 4 cortical regions that show high tau deposition at autopsy[35,36] (superior frontal, precentral, postcentral, supplementary motor area), as well as 2 cortical regions that are typically relatively unaffected pathologically in PSP (entorhinal cortex and occipital lobe).

Statistical Analysis

For each subject, we calculated the annualized change of tau-PET, defined as follow-up SUVR minus baseline SUVR divided by time in years. We summarized the annual change measures by reporting the mean and 95% CI. To investigate the differences in annualized change between PSP and control subjects across the 15 regions of interest, we calculated the area under the receiver operating characteristic curve (AUROC), a nonparametric effect-size measure that is independent of the underlying scales of the data.[37] In general, the higher the AUROC estimates, the better is the discrimination between groups. To correct for age, for each ROI, we fitted a linear regression between tau SUVR and age. The residual values from the regression were used for the AUROC analysis. *P* values and 95% confidence intervals for the regions of interest were based on the link between AUROC and the Mann–Whitney *U* statistic.[38] The *P* values were also adjusted for multiple comparisons using false discovery rate correction. A nonparametric analysis approach was appropriate for our data because the [^{18}F]AV-1451 estimates were not normally distributed. However, for comparison purposes, we also provide the parametric Cohen's D effect-size metric. The Cohen's d estimate was the difference in means scaled by the residual standard deviation from an age-adjusted linear regression model. We investigated differences in annualized midbrain volume change between PSP and controls using this same analytical approach. Spearman's correlations were calculated between annualized change in the PSPRS and annualized change in imaging metrics, and between baseline and annualized change measures for [^{18}F]AV-1451. Sample-size requirements per treatment arm for a placebo-controlled treatment trial were estimated for rates of midbrain atrophy, change in PSPRS over time,

and change in the top [^{18}F]AV-1451 measures. Estimated sample sizes needed for PSP subjects to detect a 20% reduction in the rate of change based on 80% and 90% power, 2-sided, 2-sample *t* test, with an α of 0.05 were calculated. Statistical analyses were performed using PET scans that had undergone PVC, and also repeated using PET scans without PVC. The statistical analyses were performed using R version 3.4.1.

Results

Evaluation of Subject-Level [^{18}F]AV-1451 Change

Tau-PET SUVRs across all regions are shown for each scan within each subject in Figure 1. The SUVR profile across regions remains relatively consistent over time in all subjects. However, the regional patterns of change over time varied across subjects. Subject 13 (Supplemental Fig. 1) showed increases in uptake over time across nearly all cortical and subcortical regions. Patterns of increased uptake predominantly in the dentate nucleus of the cerebellum and brain stem regions were observed in subjects 1, 2, 4, 8, and 15, with increases observed in frontal regions in subjects 3, 10, 11, and 12. Subjects 6 and 16 (Supplemental Fig. 1) showed subtle decreases in uptake in the midbrain, dentate nucleus of the cerebellum, and putamen, with subject 6 also showing decreases in frontotemporal regions, similar to subject 7. Regional profiles were very similar when using PET scans without PVC.

Regional Comparisons of PSP Patients and Controls

Rate of midbrain atrophy on 3 T MR imaging was significantly increased in the PSP subjects compared with controls, with an AUROC estimate of 0.93 to differentiate the 2 groups (Table 2). In the [^{18}F]AV-1451 analysis, the midbrain, pallidum, and precentral cortex showed significantly increased rates of uptake in PSP compared with controls, with AUROCs ranging from 0.75 to 0.79 (Table 2). The dentate nucleus of the cerebellum and subthalamic nucleus also showed trends for increased rates of uptake in PSP compared with controls (AUROCs, 0.71 and 0.70), but these results did not survive correction for multiple comparisons. AUROC estimates were very similar when age effects were removed. In the analysis without PVC, the pallidum, precentral cortex, dentate nucleus of the cerebellum, and midbrain showed significantly increased rates of [^{18}F]AV-1451 uptake in PSP compared with controls, with AUROCs ranging from 0.71 to 0.76, with trends for increased rates of uptake in the subthalamic nucleus and substantia nigra (AUROCs, 0.69 and 0.68); see Supplemental Table 1.

Correlations With Baseline Uptake and Disease Severity in PSP

Change in midbrain volume showed a reasonably strong correlation with change in PSPRS over the 12-month interval (r = -0.48, P = 0.09). However, we did not observe any significant correlations between change in [^{18}F]AV-1451 uptake over time for the midbrain, precentral cortex, dentate nucleus of the cerebellum, or pallidum and change in the PSPRS (Fig. 2). We also did not see any significant associations between baseline [^{18}F]AV-1451 uptake and change in [^{18}F]AV-1451 uptake over time for these regions (Fig. 2). These [^{18}F]AV-1451 results remained the same in the analysis without PVC.

Sample-Size Estimates

The smallest sample-size estimates were achieved with rate of midbrain volume followed by rate of change in the PSPRS (Table 3). Both these metrics provided smaller sample-size estimates than the [^{18}F]AV-1451 measures. Within the [^{18}F]AV-1451 measures, sample sizes for the top 4 regions were smaller with PVC than without PVC, with the smallest achieved with change in the pallidum.

Discussion

This regional longitudinal analysis of [^{18}F]AV-1451 tau-PET binding showed evidence that [^{18}F]AV-1451 uptake increased over time in the pallidum, precentral cortex, dentate nucleus of the cerebellum, and midbrain in PSP. However, the effect sizes for these measures were smaller than those observed for rate of midbrain atrophy; only midbrain atrophy, and not [^{18}F]AV-1451 uptake, correlated with disease severity, and midbrain atrophy provided smaller sample-size estimates for clinical treatment trials. This suggests that rate of midbrain atrophy would be a more clinically relevant measure of PSP progression than [^{18}F]AV-1451 and thus more useful as a longitudinal biomarker for clinical treatment trials in PSP.

The 4 key regions that showed the most robust evidence for increased uptake of [^{18}F]AV-1451 over time in PSP are typically affected by tau pathology and neurodegeneration in PSP.[39-41] The pallidum, midbrain, and dentate nucleus of the cerebellum have also consistently shown elevated [^{18}F]AV-1451 in PSP compared with controls in cross-sectional studies.[16-18,20,21] Elevated uptake in cortical regions including the precentral cortex has been observed in some cross-sectional studies,[20,21] although not all,[17,18] and uptake was typically not as striking as that observed in the subcortical structures.[20,21] Our findings suggest that the precentral cortex may be actively accumulating tau at this point in the disease, perhaps reflecting disease spread from

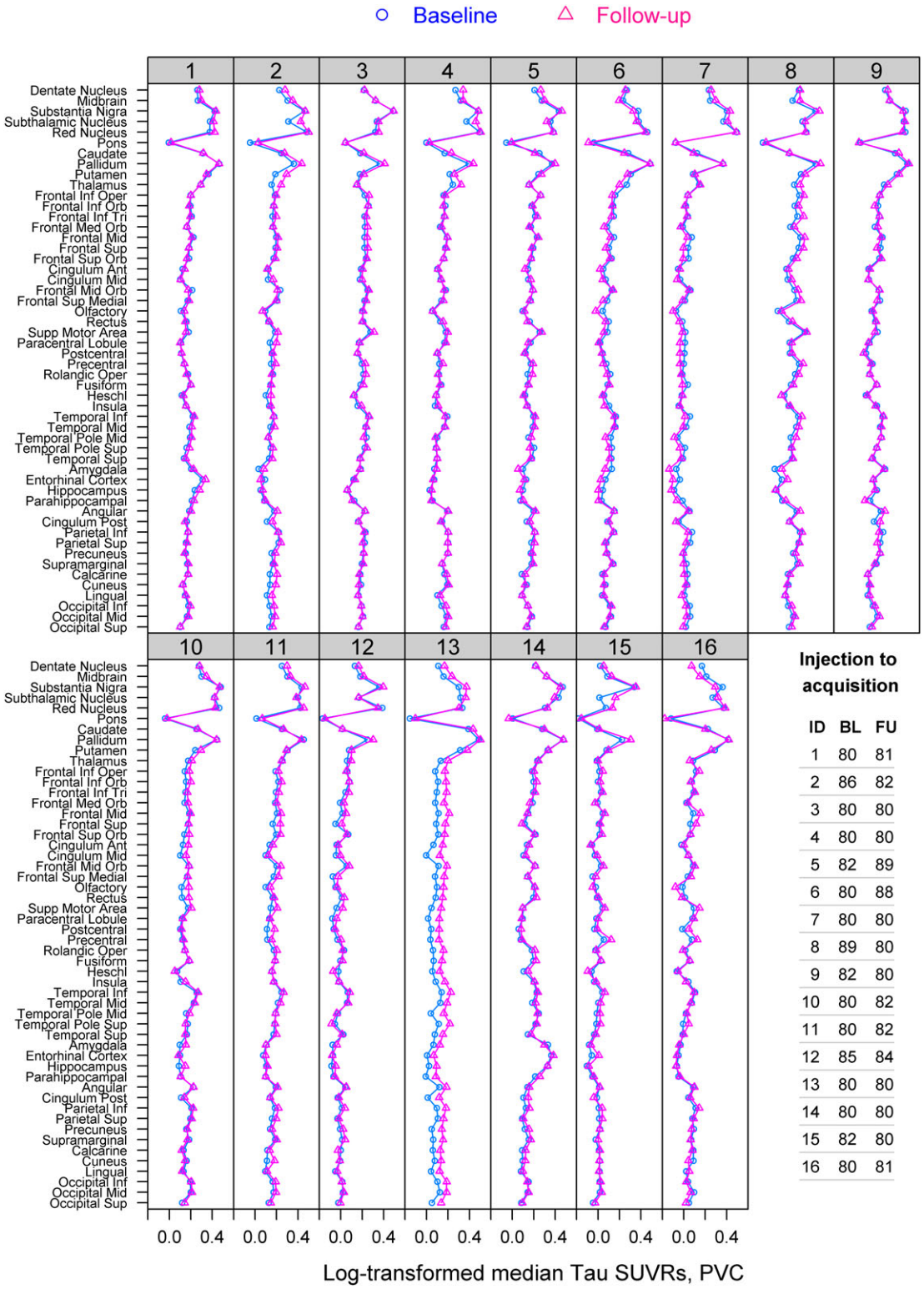

FIG. 1. [^{18}F]AV-1451 SUVR regional profiles for baseline (BL) and follow-up (FU) scans of the 16 PSP subjects. Time from injection of [^{18}F]AV-1451 to PET acquisition (minutes) is shown for each scan for each subject.

subcortical structures to the cortex. However, the amount a subject changes over time in these regions is not related to the amount of uptake at baseline, perhaps telling us something biological about disease spread or reflecting noise in the measurements. The regions of interest placed on the subthalamic nucleus and substantia nigra also performed reasonably well in our longitudinal analysis, likely reflecting that they are

TABLE 2. Comparisons of change measures in PSP and controls

	Annualized change, mean (95% CI)		AUROC			Cohen's d[a]
	PSP (n = 16)	Control (n = 39)	Est (95% CI)	*P*	Est (95% CI) removed age effect	Est (95% CI)
MRI volume						
Midbrain	−0.25 (−0.32 to −0.18)	−0.03(−0.07 to 0.003)	0.93 (0.79 to 0.98)	< 0.001[b]	0.92 (0.78 to 0.97)	−1.87 (1.33 to 2.71)
[18F]AV-1451 uptake						
Midbrain	0.04 (0.01 to 0.06)	−0.009 (−0.02 to 0.003)	0.79 (0.62 to 0.89)	< 0.001[b]	0.79 (0.62 to 0.89)	1.07 (0.40 to 1.97)
Pallidum	0.07 (0.03 to 0.11)	−0.004 (−0.02 to 0.01)	0.76 (0.60 to 0.87)	0.002[b]	0.76 (0.60 to 0.87)	1.10 (0.48 to 1.92)
Precentral	0.03 (0.009 to 0.05)	−0.001 (−0.009 to 0.008)	0.75 (0.58 to 0.86)	0.003[b]	0.74 (0.57 to 0.85)	0.98 (0.32 to 1.85)
Dentate nucleus	0.03 (0.003 to 0.06)	−0.003 (−0.02 to 0.01)	0.71 (0.54 to 0.83)	0.01	0.70 (0.53 to 0.83)	0.65 (0.05 to 1.39)
Subthalamic nucleus	0.05 (0.001 to 0.11)	−0.01 (−0.03 to 0.009)	0.70 (0.53 to 0.83)	0.02	0.70 (0.53 to 0.82)	0.86 (0.17 to 1.65)
Supplementary motor area	0.02 (0.002 to 0.05)	0.0004 (−0.009 to 0.01)	0.67 (0.50 to 0.80)	0.05	0.67 (0.50 to 0.80)	0.71 (0.05 to 1.56)
Thalamus	0.02 (−0.006 to 0.05)	−0.004 (−0.02 to 0.007)	0.67 (0.50 to 0.80)	0.06	0.67 (0.50 to 0.80)	0.66 (−0.04 to 1.47)
Occipital	0.01 (−0.001 to 0.03)	−0.001 (−0.009 to 0.007)	0.66 (0.49 to 0.79)	0.06	0.66 (0.49 to 0.79)	0.55 (−0.03 to 1.23)
Substantia nigra	0.02 (−0.03 to 0.070)	−0.02 (−0.04 to 0.005)	0.66 (0.49 to 0.79)	0.07	0.66 (0.49 to 0.79)	0.51 (−0.13 to 1.25)
Putamen	0.03 (0.002 to 0.06)	0.005 (−0.009 to 0.02)	0.66 (0.49 to 0.79)	0.07	0.64 (0.47 to 0.78)	0.59 (−0.06 to 1.30)
Caudate	0.02 (−0.01 to 0.04)	−0.004 (−0.02 to 0.01)	0.63 (0.46 to 0.77)	0.14	0.63 (0.47 to 0.77)	0.45 (−0.16 to 1.11)
Postcentral	0.02 (−0.003 to 0.03)	0.001 (−0.008 to 0.009)	0.62 (0.45 to 0.76)	0.16	0.61 (0.44 to 0.75)	0.53 (−0.10 to 1.22)
Red nucleus	0.01 (−0.03 to 0.06)	−0.02 (−0.04 to 0.002)	0.61 (0.44 to 0.75)	0.21	0.61 (0.44 to 0.75)	0.45 (−0.21 to 1.16)
Entorhinal cortex	0.007 (−0.02 to 0.03)	−0.004 (−0.02 to 0.007)	0.58 (0.42 to 0.73)	0.34	0.59 (0.42 to 0.73)	0.31 (−0.33 to 0.98)
Superior frontal	0.02 (−0.006 to 0.04)	−0.001 (−0.01 to 0.009)	0.58 (0.42 to 0.73)	0.34	0.60 (0.43 to 0.74)	0.54 (−0.13 to 1.27)

[a]Difference in means scaled by residual standard deviation from an age-adjusted linear regression model.
[b]Still statistically significant (adjusted *P* or q < 0.05) after controlling for false discovery rate.

both capturing the elevated signal observed in the midbrain in PSP subjects. However, neither performed as well as the midbrain region of,interest, which is larger and subsumes both these brain stem nuclei.

Individual patterns of change in uptake did show variability, however, with some subjects showing evidence for increased [^{18}F]AV-1451 uptake, but others showing decreased uptake over time. We also had a subject who stood out because increased uptake was observed across all regions of the brain. This variability likely reduced power in the group-level results. Of course, the difficulty in interpreting these longitudinal tau-PET results is that we have no biologic marker documenting how tau burden changes over the course of this disease. Pathological studies can only sample 1 time at the end of the disease. Although one might assume that tau pathology gradually accumulates over the course of the disease, it has been found that some oligodendroglial tau pathology actually decreases with disease duration in PSP.[42] In addition, the accumulated tau burden at any point may be partially offset by physiological degradation of tau aggregates.[43] The variability we observed across subjects could reflect this biological heterogeneity. Furthermore, we have no current assurances that [^{18}F]AV-1451 tau-PET is providing an accurate measure of the burden of underlying 4R tau in PSP. Instead, it may reflect off-target binding to something other than 4R tau. If this is the case, then our data suggest that whatever the off-target binding site is, it does increase over time in PSP.

Despite observing regions with increasing [^{18}F]AV-1451 uptake over time, it was clear that [^{18}F]AV-1451 did not perform as well as midbrain volume as a disease biomarker in PSP. An important aspect of a disease biomarker is that it should relate to progression of the disease. This is the case for rate of midbrain atrophy, which we found to correlate to change over time on the PSPRS in our cohort. Others have similarly observed good correlations between midbrain measures and disease severity in PSP.[9,44-46] However, we did not observe any correlation between decline in disease severity and longitudinal measures of [^{18}F]AV-1451. Furthermore, sample-size estimates for clinical trials were much smaller for rate of midbrain volume compared with the [^{18}F]AV-1451 measures, with only 94 subjects required per treatment arm with rate of midbrain volume loss for a trial with 80% power to detect a 20% treatment effect. These estimates are roughly in line with those obtained in previous studies for rate of midbrain volume change.[7-9] In comparison, 521 subjects per treatment arm would be required when using the pallidum, which was the best of the [^{18}F]AV-1451 measures. Of note, we found that the sample-size estimates were the smallest and the effect sizes of the difference between PSP and controls were the largest, when using PVC data compared with estimates without PVC. There is a current lack of consensus in the field concerning the value of PVC in [^{18}F]AV-1451 analysis, but in this situation it does increase power slightly. Sample-size estimates from the PSPRS were also smaller than those from the [^{18}F]AV-1451 measures, although it did not perform as well as rate of midbrain volume, consistent with previous findings.[8,9]

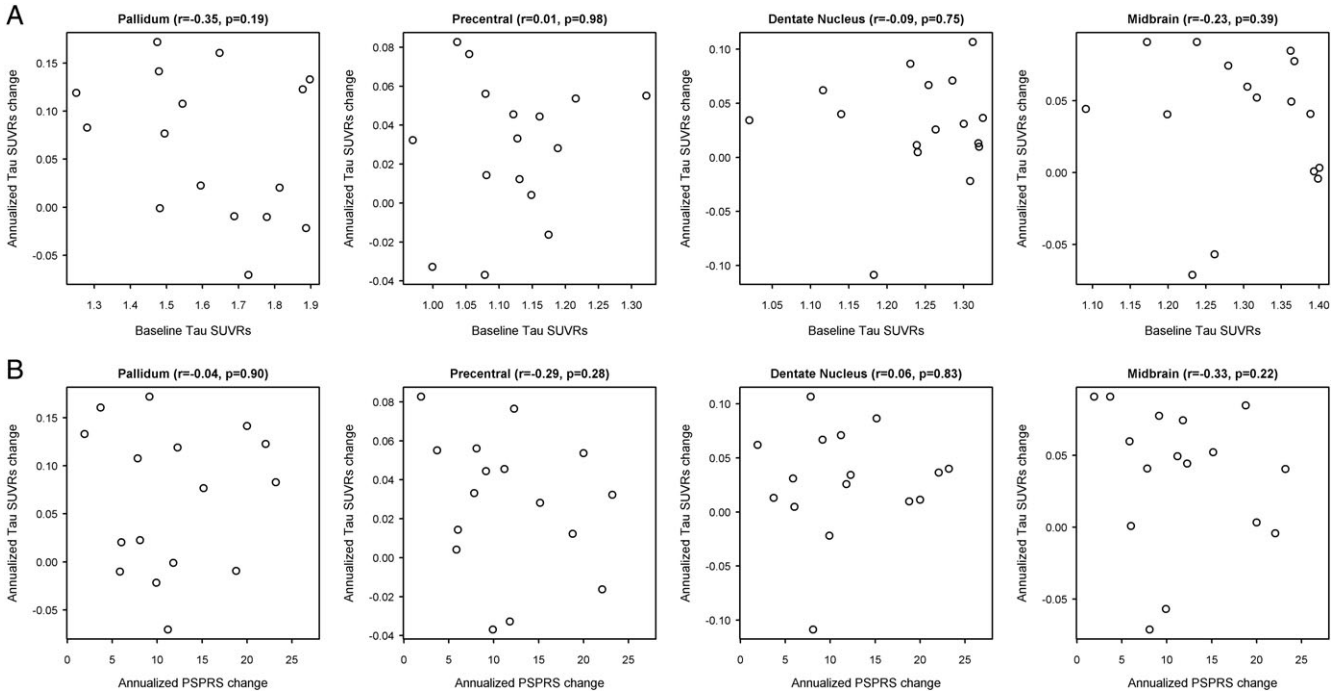

FIG. 2. Scatterplots showing the relationship (A) between annualized change in [^{18}F]AV-1451 measures and baseline [^{18}F]AV-1451 and (B) between annualized change in [^{18}F]AV-1451 and annualized change in PSP Rating Scale (PSPRS).

Strengths of our study include that our cohort consisted of 3 clinical variants of PSP, which may increase generalizability to other PSP cohorts, and our findings were very similar in the analysis with and without PVC, with the same top set of regions identified in both analyses. However, our findings may not generalize to other variant syndromes of PSP that we did not include, and the number of subjects was too small to allow us to perform analyses across the different clinical variants. Future studies with larger numbers of subjects will need to determine whether patterns of change in [^{18}F]AV-1451 differ across the clinical variants of PSP. It is important to also acknowledge that our results may not generalize to patients earlier in the disease course. The longitudinal trajectory of [^{18}F]AV-1451 changes has not yet been established in PSP, and it is quite possible that rates of change may be greatest in earlier disease stages and could perform better than MRI measures in this phase of the disease. In addition, a limitation of the study is our necessary use of late-uptake SUVR images. SUVR images are less reliable than PET quantification methods using full-dynamic acquisitions, and longitudinal studies using SUVR can be confounded by differences in brain perfusion.[47] However, late-uptake scans with SUVR remain the most common method for PSP studies because of the large increase in cost, patient burden, and scanner access required for full-dynamic acquisitions. Performing full-dynamic scans for AV-1451 would require more than 100 minutes of scan time, rather than 20 minutes, and this was not feasible for our study.

Our study provides some evidence that [^{18}F]AV-1451 uptake changes over time in subjects with PSP. However, given the variability we observed in longitudinal

TABLE 3. Estimated sample size estimates per treatment arm in a clinical trial to detect a reduction in each longitudinal outcome variable in PSP

Outcome variable	PVC		No PVC	
	80% Power	90% Power	80% Power	90% Power
Midbrain volume	94	125	NA	NA
PSP Rating Scale	165	220	NA	NA
Pallidum [^{18}F]AV-1451	521	697	551	737
Precentral [^{18}F]AV-1451	626	837	867	1160
Midbrain [^{18}F]AV-1451	741	992	2105	2817
Dentate nucleus of the cerebellum [^{18}F]AV-1451	1126	1507	1094	1464

Data are shown at 80% and 90% power for a potential 20% reduction in each outcome. [^{18F}]AV-1451 measures are shown both without and with partial volume correction (PVC).

change patterns in [^{18}F]AV-1451 and issues with how our results generalize to other disease stages, it will be important for in vivo [^{18}F]AV-1451 findings to be further validated at autopsy and in other PSP cohorts, particularly in a range of subjects at different stages of the disease.

Acknowledgments: We acknowledge AVID Radiopharmaceuticals for provision of the AV-1451 precursor, chemistry production advice and oversight, and FDA regulatory cross-filing permission and documentation needed for this work.

References

1. Steele JC, Richardson JC, Olszewski J. Progressive supranuclear palsy. a heterogeneous degeneration involving the brain stem, basal ganglia and cerebellum with vertical gaze and pseudobulbar palsy, nuchal dystonia and dementia. Arch Neurol 1964;10:333-359.
2. Hoglinger GU, Respondek G, Stamelou M, et al. Clinical diagnosis of progressive supranuclear palsy: The movement disorder society criteria. Mov Disord 2017;32(6):853-864.
3. Josephs KA, Hodges JR, Snowden J, et al. Neuropathological background of phenotypical variability in frontotemporal dementia. Acta Neuropathol 2011;122(2):137-153.
4. Osaki Y, Ben-Shlomo Y, Lees AJ, et al. Accuracy of clinical diagnosis of progressive supranuclear palsy. Mov Disord 2004;19(2):181-189.
5. Respondek G, Roeber S, Kretzschmar H, et al. Accuracy of the National Institute for Neurological Disorders and Stroke/Society for Progressive Supranuclear Palsy and neuroprotection and natural history in Parkinson plus syndromes criteria for the diagnosis of progressive supranuclear palsy. Mov Disord 2013;28(4):504-509.
6. Whitwell JL, Hoglinger GU, Antonini A, et al. Radiological biomarkers for diagnosis in PSP: Where are we and where do we need to be? Mov Disord 2017;32(7):955-971.
7. Paviour DC, Price SL, Lees AJ, Fox NC. MRI derived brain atrophy in PSP and MSA-P. Determining sample size to detect treatment effects. J Neurol 2007;254(4):478-481.
8. Whitwell JL, Xu J, Mandrekar JN, Gunter JL, Jack CR Jr, Josephs KA. Rates of brain atrophy and clinical decline over 6 and 12-month intervals in PSP: determining sample size for treatment trials. Parkinsonism Relat Disord 2012;18(3):252-256.
9. Hoglinger GU, Schope J, Stamelou M, et al. Longitudinal magnetic resonance imaging in progressive supranuclear palsy: A new combined score for clinical trials. Mov Disord 2017;32(6):842-852.
10. Chien DT, Bahri S, Szardenings AK, et al. Early clinical PET imaging results with the novel PHF-tau radioligand [F-18]-T807. J Alzheimers Dis 2013;34(2):457-468.
11. Xia CF, Arteaga J, Chen G, et al. [(18)F]T807, a novel tau positron emission tomography imaging agent for Alzheimer's disease. Alzheimers Dement 2013;9(6):666-676.
12. Lowe VJ, Curran G, Fang P, et al. An autoradiographic evaluation of AV-1451 Tau PET in dementia. Acta Neuropathol Commun 2016;4(1):58.
13. Marquie M, Normandin MD, Vanderburg CR, et al. Validating novel tau positron emission tomography tracer [F-18]-AV-1451 (T807) on postmortem brain tissue. Ann Neurol 2015;78(5):787-800.
14. Sander K, Lashley T, Gami P, et al. Characterization of tau positron emission tomography tracer [18F]AV-1451 binding to postmortem tissue in Alzheimer's disease, primary tauopathies, and other dementias. Alzheimers Dement 2016;12(11):1116-1124.
15. Smith R, Scholl M, Honer M, Nilsson CF, Englund E, Hansson O. Tau neuropathology correlates with FDG-PET, but not AV-1451-PET, in progressive supranuclear palsy. Acta Neuropathol 2017;133(1):149-151.
16. Smith R, Schain M, Nilsson C, et al. Increased basal ganglia binding of 18 F-AV-1451 in patients with progressive supranuclear palsy. Mov Disord 2017;32(1):108-114.
17. Cho H, Choi JY, Hwang MS, et al. Subcortical 18 F-AV-1451 binding patterns in progressive supranuclear palsy. Mov Disord 2017;32(1):134-140.
18. Passamonti L, Vazquez Rodriguez P, Hong YT, et al. 18F-AV-1451 positron emission tomography in Alzheimer's disease and progressive supranuclear palsy. Brain 2017;140(3):781-791.
19. Whitwell JL, Ahlskog JE, Tosakulwong N, et al. Pittsburgh Compound B and AV-1451 positron emission tomography assessment of molecular pathologies of Alzheimer's disease in progressive supranuclear palsy. Parkinsonism Relat Disord 2018;48:3-9.
20. Whitwell JL, Lowe VJ, Tosakulwong N, et al. [18 F]AV-1451 tau positron emission tomography in progressive supranuclear palsy. Mov Disord 2017;32(1):124-133.
21. Schonhaut DR, McMillan CT, Spina S, et al. (18) F-flortaucipir tau positron emission tomography distinguishes established progressive supranuclear palsy from controls and Parkinson disease: A multicenter study. Ann Neurol 2017;82(4):622-634.
22. Golbe LI, Ohman-Strickland PA. A clinical rating scale for progressive supranuclear palsy. Brain 2007;130(Pt 6):1552-1565.
23. Whitwell JL, Master AV, Avula R, et al. Clinical correlates of white matter tract degeneration in progressive supranuclear palsy. Arch Neurol 2011;68(6):753-760.
24. Nasreddine ZS, Phillips NA, Bedirian V, et al. The Montreal Cognitive Assessment, MoCA: a brief screening tool for mild cognitive impairment. J Am Geriatr Soc 2005;53(4):695-699.
25. Dubois B, Slachevsky A, Litvan I, Pillon B. The FAB: a Frontal Assessment Battery at bedside. Neurology 2000;55(11):1621-1626.
26. Jack CR Jr, Wiste HJ, Weigand SD, et al. Defining imaging biomarker cut points for brain aging and Alzheimer's disease. Alzheimers Dement 2017;13(3):205-216.
27. Meltzer CC, Kinahan PE, Greer PJ, et al. Comparative evaluation of MR-based partial-volume correction schemes for PET. J Nucl Med 1999;40(12):2053-2065.
28. Ashburner J, Friston KJ. Unified segmentation. Neuroimage 2005;26(3):839-851.
29. Schwarz CG, Gunter JL, Ward CP, et al. The Mayo Clinic Adult Lifespan Template: better quantification across the lifespan. Alzheimers Dement 2017;13(7, Supplement):P792.
30. Botha H, Whitwell JL, Madhaven A, Senjem ML, Lowe V, Josephs KA. The pimple sign of progressive supranuclear palsy syndrome. Parkinsonism Relat Disord 2014;20(2):180-185.
31. Fujiwara A, Yoshida T, Otsuka T, et al. Midbrain volume increase in patients with panic disorder. Psychiatry Clin Neurosci 2011;65(4):365-373.
32. Ewert S, Plettig P, Li N, et al. Toward defining deep brain stimulation targets in MNI space: A subcortical atlas based on multimodal MRI, histology and structural connectivity. Neuroimage 2018;170:271-282.
33. Avants BB, Epstein CL, Grossman M, Gee JC. Symmetric diffeomorphic image registration with cross-correlation: evaluating automated labeling of elderly and neurodegenerative brain. Med Image Anal 2008;12(1):26-41.
34. Lowe VJ, Wiste HJ, Senjem ML, et al. Widespread brain tau and its association with ageing, Braak stage and Alzheimer's dementia. Brain 2018;141(1):271-287.
35. Dickson DW, Hauw JJ, Agid Y, Litvan I. Progressive supranuclear palsy and corticobasal degeneration. In: Dickson D, Weller RO, eds. Neurodegeneration: the Molecular Pathology of Dementia and Movement Disorders. 2nd ed. Chichester, UK: Wiley-Blackwell; 2011.
36. Hauw JJ, Daniel SE, Dickson D, et al. Preliminary NINDS neuropathologic criteria for Steele-Richardson-Olszewski syndrome (progressive supranuclear palsy). Neurology 1994;44(11):2015-2019.
37. Acion L, Peterson JJ, Temple S, Arndt S. Probabilistic index: an intuitive non-parametric approach to measuring the size of treatment effects. Stat Med 2006;25(4):591-602.
38. Newcombe RG. Confidence intervals for an effect size measure based on the Mann-Whitney statistic. Part 1: general issues and tail-area-based methods. Stat Med 2006;25(4):543-557.

39. Josephs KA, Whitwell JL, Dickson DW, et al. Voxel-based morphometry in autopsy proven PSP and CBD. Neurobiol Aging 2008; 29(2):280-289.

40. Dickson DW, Ahmed Z, Algom AA, Tsuboi Y, Josephs KA. Neuropathology of variants of progressive supranuclear palsy. Curr Opin Neurol 2010;23(4):394-400.

41. Whitwell JL, Avula R, Master A, et al. Disrupted thalamocortical connectivity in PSP: a resting-state fMRI, DTI, and VBM study. Parkinsonism Relat Disord 2011;17(8):599-605.

42. Josephs KA, Mandrekar JN, Dickson DW. The relationship between histopathological features of progressive supranuclear palsy and disease duration. Parkinsonism Relat Disord 2006;12(2):109-112.

43. Sato C, Barthelemy NR, Mawuenyega KG, et al. Tau kinetics in neurons and the human central nervous system. Neuron 2018;97(6): 1284-1298 e1287.

44. Whitwell JL, Xu J, Mandrekar J, Gunter JL, Jack CR Jr, Josephs KA. Imaging measures predict progression in progressive supranuclear palsy. Mov Disord 2012;27(14):1801-1804.

45. Dutt S, Binney RJ, Heuer HW, et al. Progression of brain atrophy in PSP and CBS over 6 months and 1 year. Neurology 2016;87(19): 2016-2025.

46. Paviour DC, Price SL, Jahanshahi M, Lees AJ, Fox NC. Longitudinal MRI in progressive supranuclear palsy and multiple system atrophy: rates and regions of atrophy. Brain 2006;129(Pt 4): 1040-1049.

47. van Berckel BN, Ossenkoppele R, Tolboom N, et al. Longitudinal amyloid imaging using 11C-PiB: methodologic considerations. J Nucl Med 2013;54(9):1570-1576.

Supporting Data

Additional Supporting Information may be found in the online version of this article at the publisher's web-site.